

Frascati, October 25, 1993

Note: **L-11**

## ALTERNATIVE INTERACTION REGION DESIGN

*M. Bassetti, C. Biscari, C. Milardi*

### INTRODUCTION

Beam focusing in storage rings is usually performed by quadrupoles, which act separately on the two transverse planes, focusing in one and defocusing in the other and keeping the two planes uncoupled.

Solenoids are often used on low energy transfer lines, where the required focusing strength is not too high and furthermore the coupling effect in the transverse plane is meaningless because of the beam circular symmetry.

In high energy rings experimental detectors use often solenoidal fields which must be compensated to avoid the resulting coupling between horizontal and vertical oscillations<sup>1,2,3</sup>.

When the beam energy is sufficiently low, like in  $\Phi$ -factories, the coupling introduced by the experimental solenoid is so strong that it becomes one of the main optical characteristics of the ring.

In DAΦNE<sup>3</sup>, for the KLOE detector, special rotation of each low beta quadrupole plus the presence of compensating superconducting solenoids provide cancellation of coupling outside the interaction region (IR).

In the Novosibirsk  $\Phi$ -factory<sup>4</sup> the solenoidal coupling is not compensated but used specifically to generate emittance in the two transverse phase spaces and to focus the round beam.

### NEW COMPENSATING METHOD

We present here a new idea for a compensating method which we have applied as an example to the DAΦNE IR which houses the second experimental detector, FINUDA<sup>5</sup>. This scheme can be thought as derived from the KLOE scheme<sup>3</sup> by interchanging the position of the quadrupole triplet and the compensator. The compensator very near the IP can have a small radius and can be placed inside the detector, so that outside the detector the coupling is already vanishing. One of the advantages with respect to the previous scheme is that coupling vanishes at all energies.

Due to the compensator short length its focusing properties in both planes are very strong (see appendix). The number of quadrupoles can be reduced to two on each side; they are placed outside the detector and match the optical functions to the arcs. Of course they do not need any rotation and are conventional.

The solution studied for FINUDA is based on the preliminary experiment design parameters, recalled in the following table.

**Table I - FI.NU.DA detector characteristics.**

Total integrated field	$B_z L_s = 3 \text{ Tm}$
Maximum field	$B_{\max} = 1.1 \text{ T}$
Total length	$L_s = 2.7 \text{ m}$
Total rotation angle	$\Theta_{\text{rot}} = 50.05^\circ$

Fig. 1 represent a sketch of the proposed FI.NU.DA. IR. Table II lists the IR element characteristics and positions.

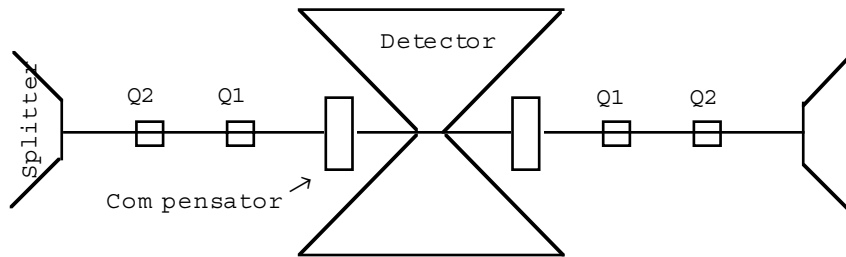


*Fig.1 - FI.NU.DA. IR sketch.*

**Table II - Half IR elements.**

Element	Position (m from IP)	Length (m)	K2 (m <sup>-2</sup> )	BLs (T m)
Detector	0.00	1.38		1.5
Compensator	0.69	0.22		1.5
Q1	1.53	0.30	-2.70000	
Q2	3.83	0.30	1.13524	

The FI.NU.DA. detector needs a region free from machine components defined by an angle of 45° starting at ~20cm from the Interaction Point (IP). This requirement is fully compatible with our proposal. Being the configuration flexible it is possible to meet eventual small experiment modifications, compatibly with the machine focusing requirements.

The computations have been performed by assuming a superconducting solenoid obtained with a 22 cm long winding. The inner radius is 6 cm and the outer 7 cm corresponding to a current density of about 550 A/mm<sup>2</sup>. Its dimensions seem compatible with the free space inside the detector. The necessary beam stay clear inside the compensator is a circle of 3.5 cm radius (see fig.3), in the hypothesis of  $10\sigma_x$  (off coupling) and  $10\sigma_y$  (full coupling) necessary for beam lifetime<sup>6</sup>, crossing angle  $\pm 15$  mrad, vertical separation @ IP of  $\pm 2.5$  mm. Therefore there is sufficient space for helium circulation, between the vacuum chamber and the solenoid winding.

The optical function behaviour in half IR are represented in fig.2 together with the beam nominal trajectory for a crossing angle of  $\pm 10$  mrad.

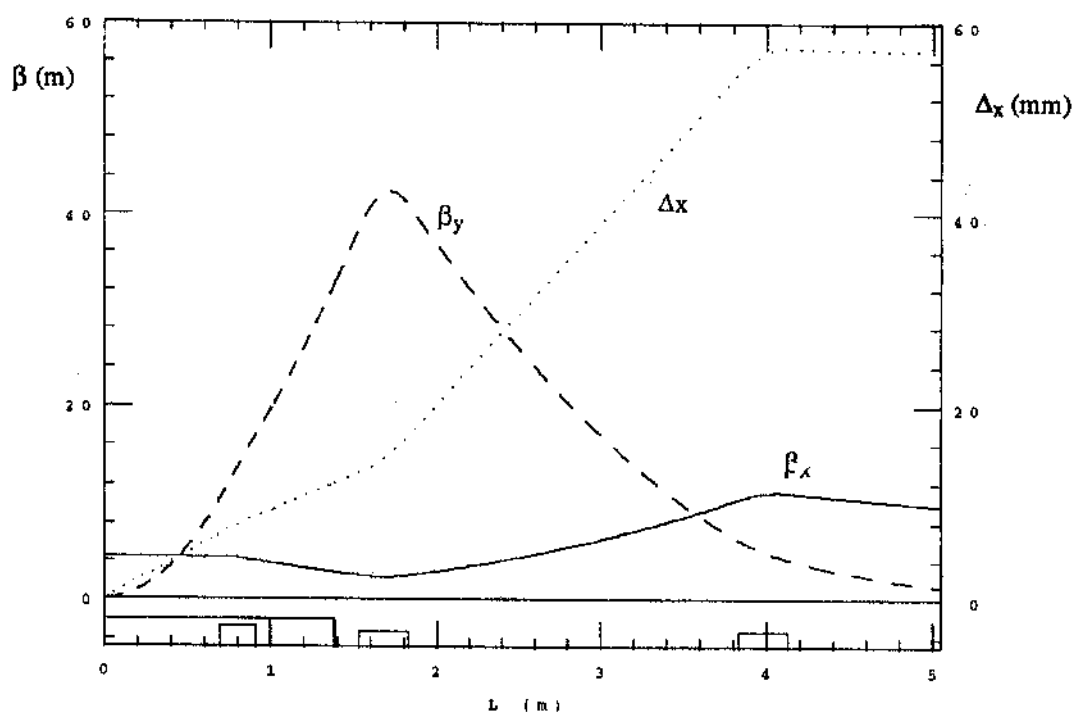


Fig.2 - Optical functions and beam central trajectories in the IR.

The first order transport matrix (4x4) at the nominal energy corresponding to half IR is reported in Table III while Table IV shows the betatron functions, the separation and the phase advances. The longitudinal magnetic field inside the detector is plotted in fig.3, together with the rotation angle of the transverse planes.

Table III - Half IR transport matrix.

0.758620	5.707345	0.000000	0.000000
-0.180469	-0.039545	0.000000	0.000000
0.000000	0.000000	-2.883339	0.200940
0.000000	0.000000	-1.376877	-0.250866

TABLE IV -Interaction Region main parameters summary.

		HORIZONTAL	VERTICAL
@ IP	$\beta$ (m)	4.5	0.045
@ IR end	$\beta$ (m)	9.827	1.272
	$\alpha$	0.666	0.942
	$\delta Q$	0.164	0.341
	D(m)*	- 0.06	
	D' *	- 0.022	
	$\Delta x$ (mm) **	71.34	
	$\Delta x'$ (mrad) **	0.049	

\* The D and D' are negative entering the SHORT and positive entering the LONG.  
\*\* for a crossing angle  $\theta = \pm 12.5$  mrad.

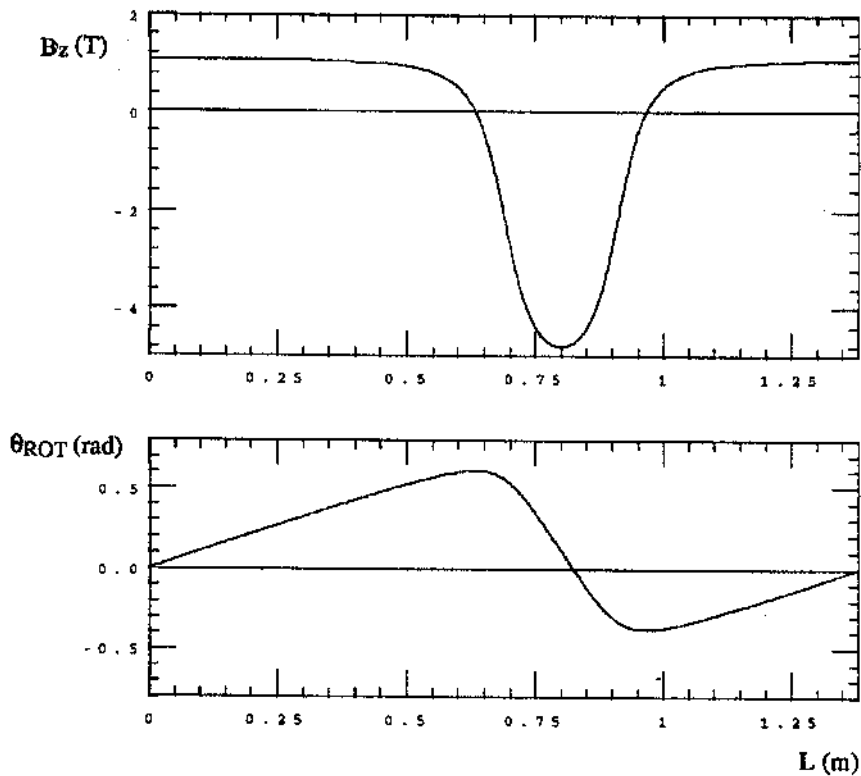


Fig.3 - Total longitudinal magnetic field in the detector zone and total rotation angle.

The required beam stay clear apertures along half IR region are shown in fig 4. They have been computed under the above described assumptions.

If the detector field should change, the compensating solenoid can be changed accordingly to compensate the variation (this is not possible in the previous scheme with quadrupoles if their relative rotation is fixed). Unfortunately this does not mean that the optics outside the detector remains unperturbed. Since the focusing effect of a solenoid (see Appendix) does not depend on the current direction, while does the rotation, lowering the compensator field to maintain the compensation, its focusing properties drastically change. It is clear that any change in the detector field has to be paid in terms of luminosity, of chromaticity, and hence of dynamic aperture, and of vacuum chamber apertures.

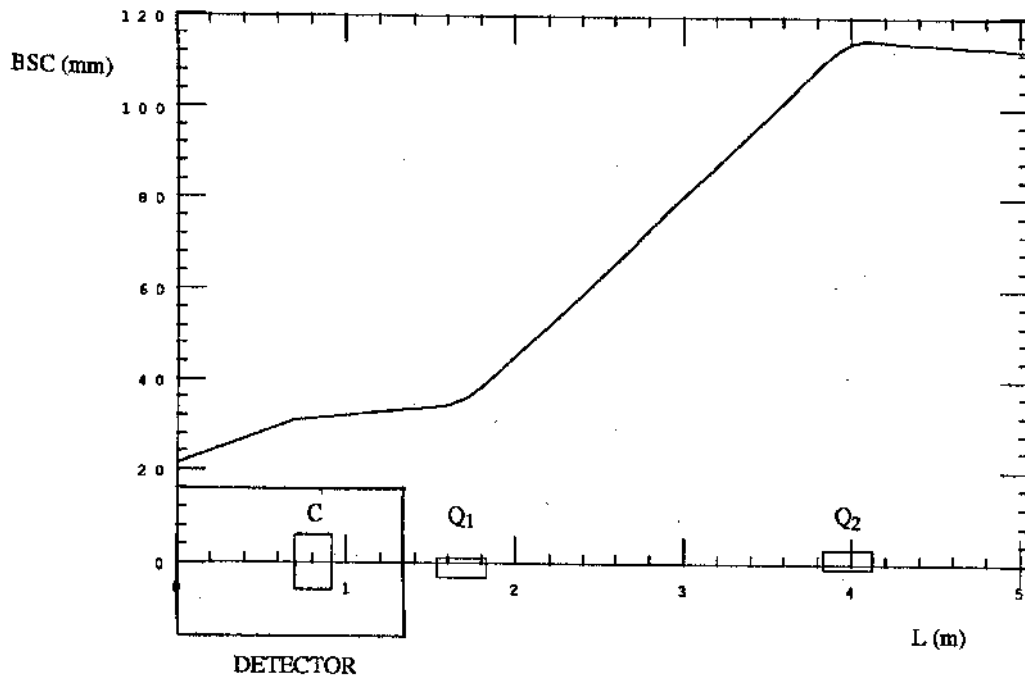


Fig.4 - Beam stay clear apertures in half IR.

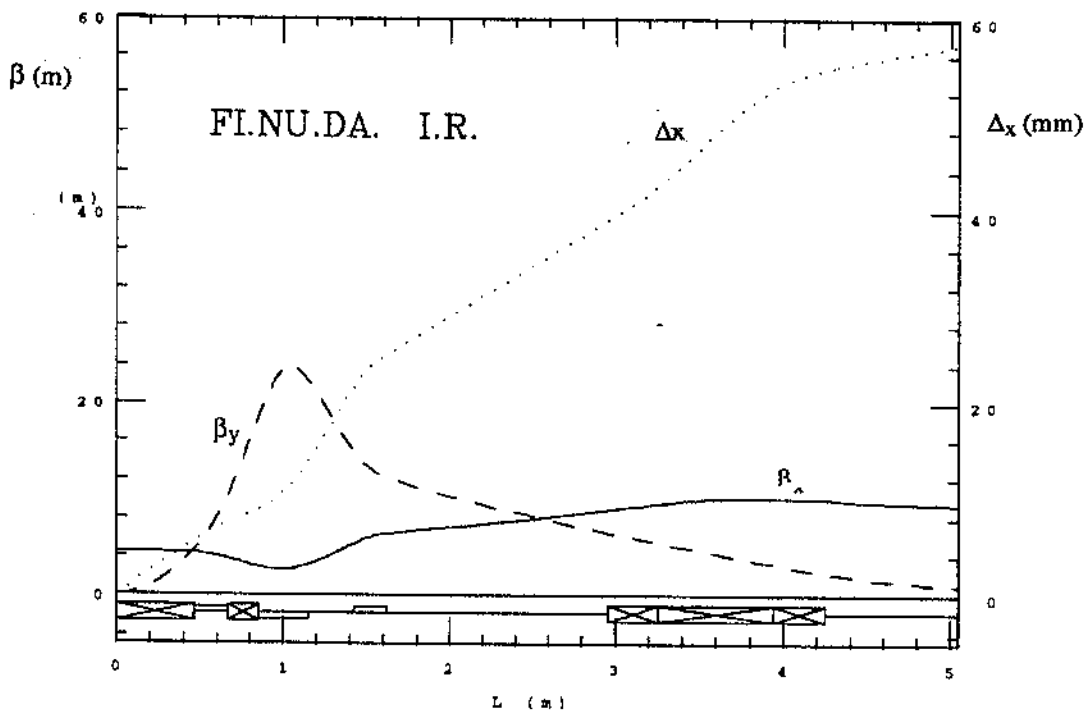


Fig.5- Optical functions and beam central trajectories in the IR with previous solution.

On the contrary the IR optics is almost unperturbed if the detector is switched off. The two compensating solenoids must be oppositely powered, at a field  $|B| = |B_c| - |B_d|$  where  $B_c$  and  $B_d$  are the normal operating fields of compensator and detector.

We report here for comparison the scheme for FINUDA<sup>7</sup> of the same type as for KLOE; three quadrupoles on each side of the IP focus the beam at the IP. They are rotated along the longitudinal axis following the rotation introduced by the detector solenoid. Two compensating superconducting solenoids compensate the integral of the longitudinal magnetic field inside the IR; the optical functions and the separation for a crossing angle of  $\pm 12.5$  mrad in half IR are plotted in fig.5.

## MAGNETIC FIELD ANALYSIS

An analysis of the magnetic properties of the system detector + compensator has been carried out, under the assumption of a constant field in the main detector solenoid with the compensator coil superimposed without any iron contribution.

Due to the cylindrical symmetry of the model the magnetic field is bidimensional and can be computed both inside and outside each solenoid. It has to be stressed that this estimate cannot be easily performed for quadrupoles, because their field is tridimensional.

The longitudinal, radial and total magnetic field profile of the small solenoid are shown in figs.6 along half detector length. Each plot shows the field on the axis and on concentric surfaces of different radius. It is interesting to notice that the longitudinal field decreases rapidly moving away from the axis:  $B_z$  is of the order of 10% of the value on axis at  $r = 10$  cm. In figs.7 the magnetic lines of force for half IR are represented without and with the detector field; it is clear that the detector field is not disturbed inside the  $45^\circ$  cone as expected.

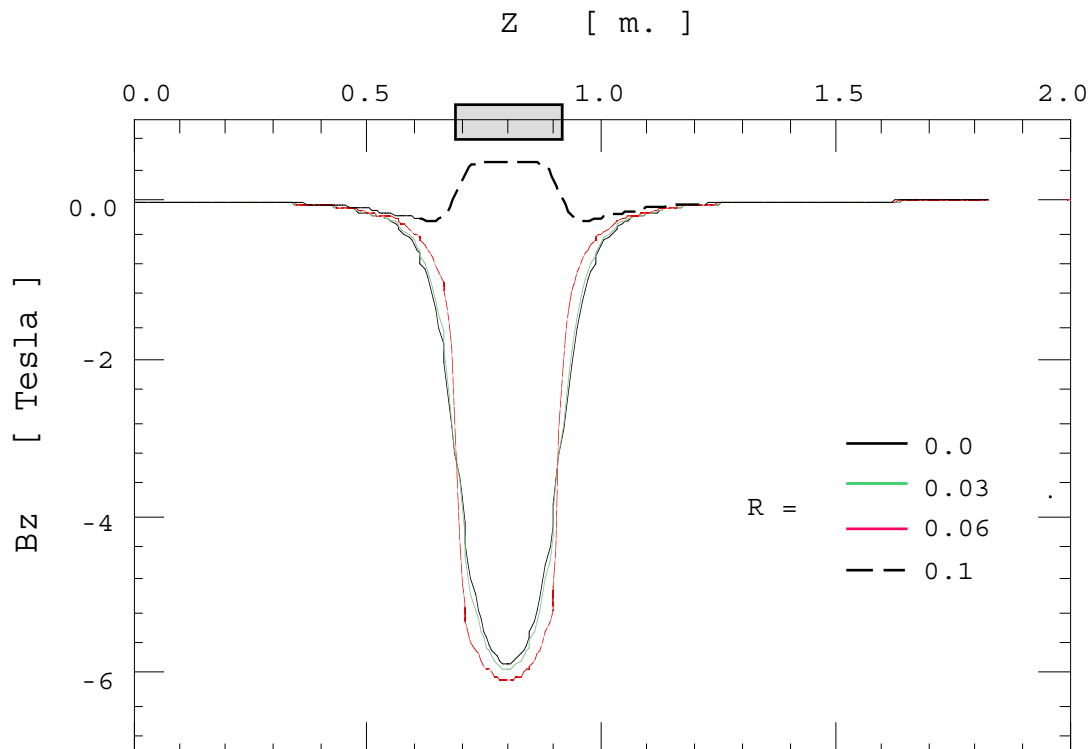


Fig.6a - Longitudinal magnetic field of the compensating solenoid along the detector length.

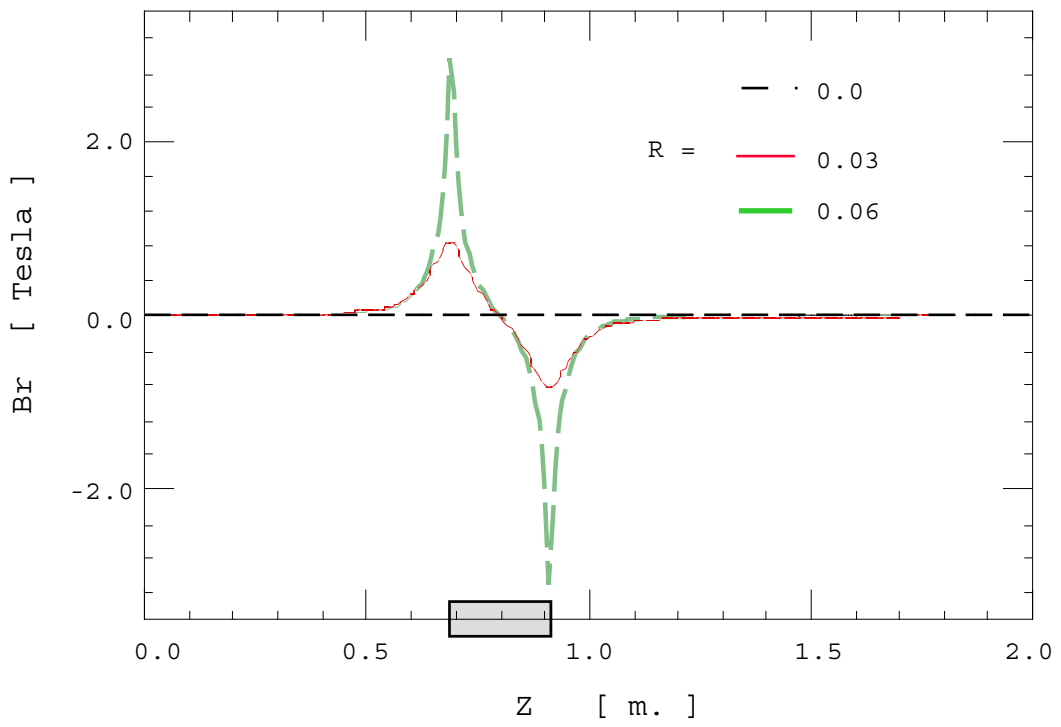


Fig.6b - Radial magnetic field of the compensating solenoid along the detector length.

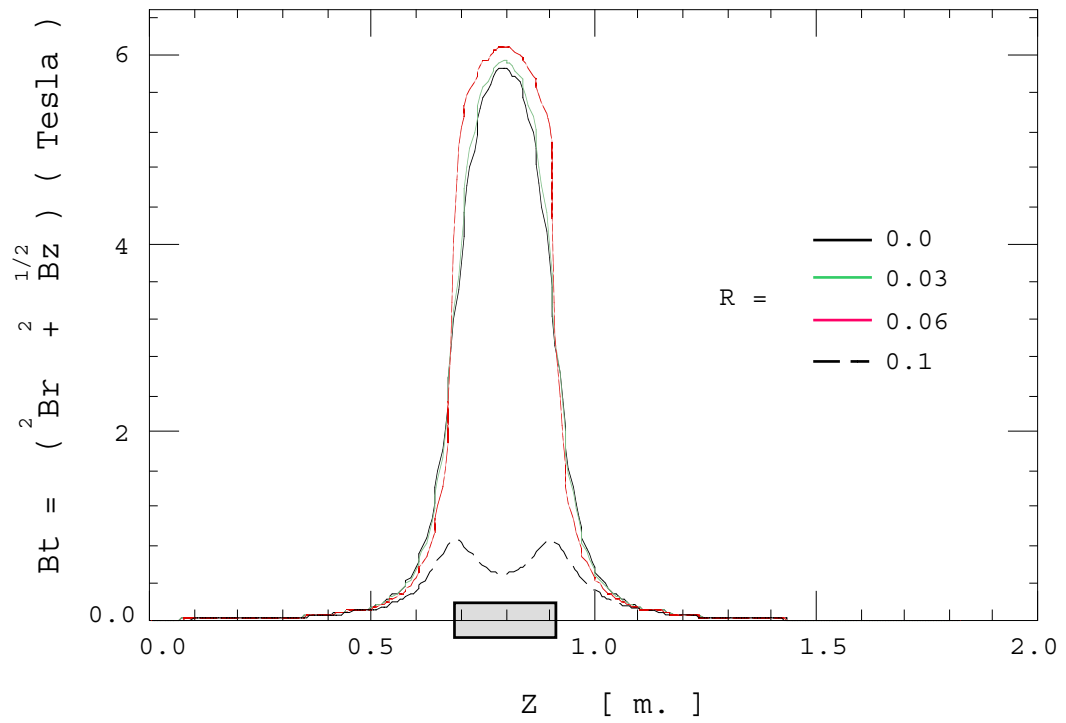


Fig.6c - Total magnetic field of the compensating solenoid along the detector length.

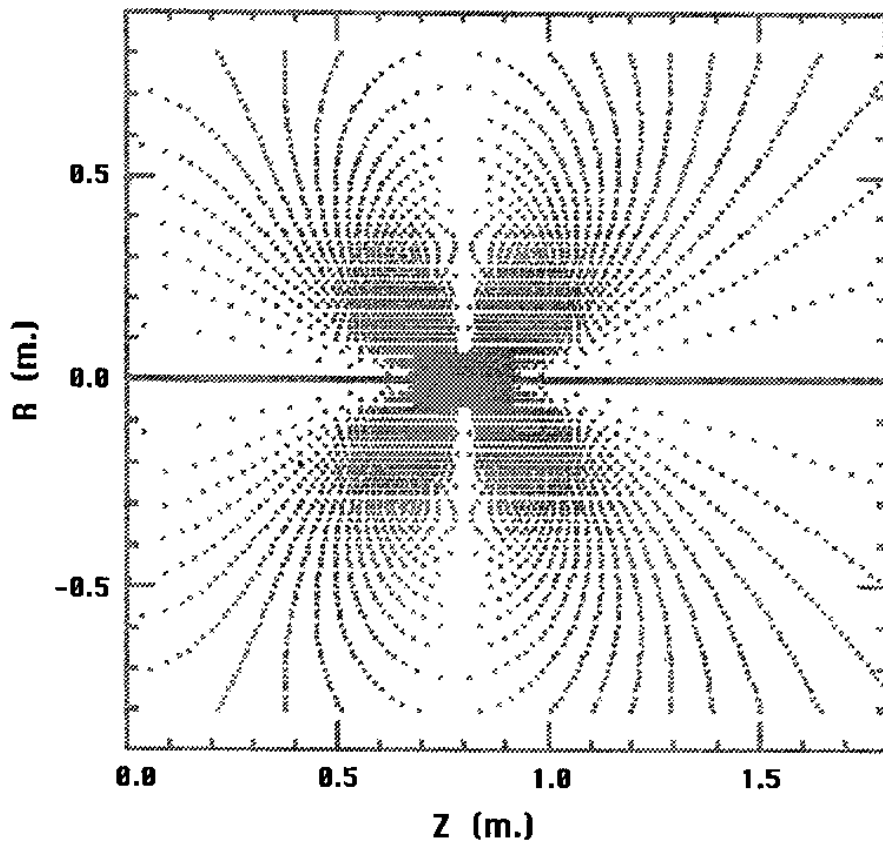


Fig.7a - Magnetic lines of force in side the detector with detector off.

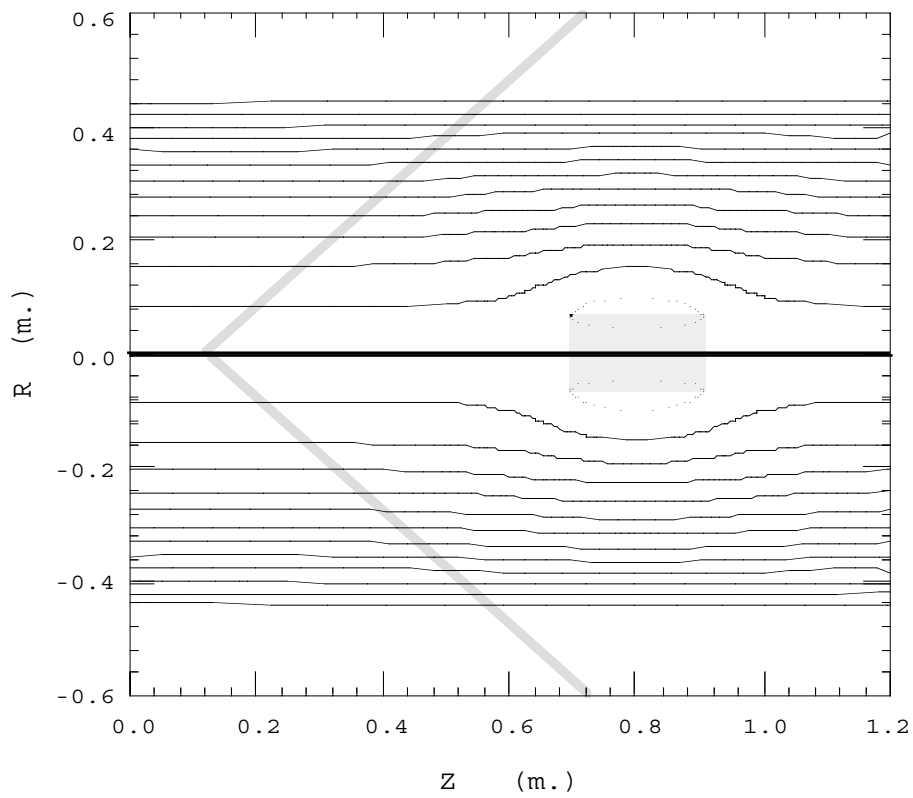


Fig.7b - Magnetic lines of force in side the detector with detector on.



## ANALYTICAL COMPUTATIONS

A tracking code has been developed where the particle trajectories are computed as solutions of the three-dimensional equations corresponding to the motion of relativistic particles inside the total magnetic field.

Solving the equations, the Jacobian around the particle trajectory has been computed and used as the transport matrix corresponding to the whole detector zone. This matrix can be used in kick codes. The same matrix can be computed by multiplication of many rectangular matrices (see appendix). We found a good agreement in the comparison between the two different approaches.

The analysis of the Jacobian around the axis verifies as expected that horizontal and vertical planes are uncoupled. The Jacobian around the actual particle trajectory, having an angle of 12.5 mrad with the axis at the IP, shows a small coupling never exceeding the project value of 1%.

It is worth pointing out that computations of this kind were never done for quadrupoles because of their difficulty.

## COMPATIBILITY WITH THE NOMINAL RING OPTICS

The total IR transfer matrix is very similar to the other IR design ones<sup>7</sup>. The optical functions at the splitter are almost the same and the separation a little larger, manageable with the splitter-corrector system.

The IR optics has been designed to keep the relative phases between sextupoles as they are in D17 (KLOE + detuned)<sup>7</sup>.

To compare the main characteristics of the optics with an already studied configuration a machine with FINUDA in the 2nd IP and the detuned lattice in the first IP has been designed. The total tunes are (5.18, 5.15).

Dynamic aperture has been computed with the DAΦNE code<sup>8</sup>, in a version which reads the transfer matrix of the detector zone for different energies and uses it in the tracking. Results are satisfactory and even better than D17 even if the chromaticity is slightly higher: (-9.0, -16.6) instead of (-8.7, -14.3).

Figs.8 represent the dynamic aperture, the tune dependence on momentum and amplitude for different energies.

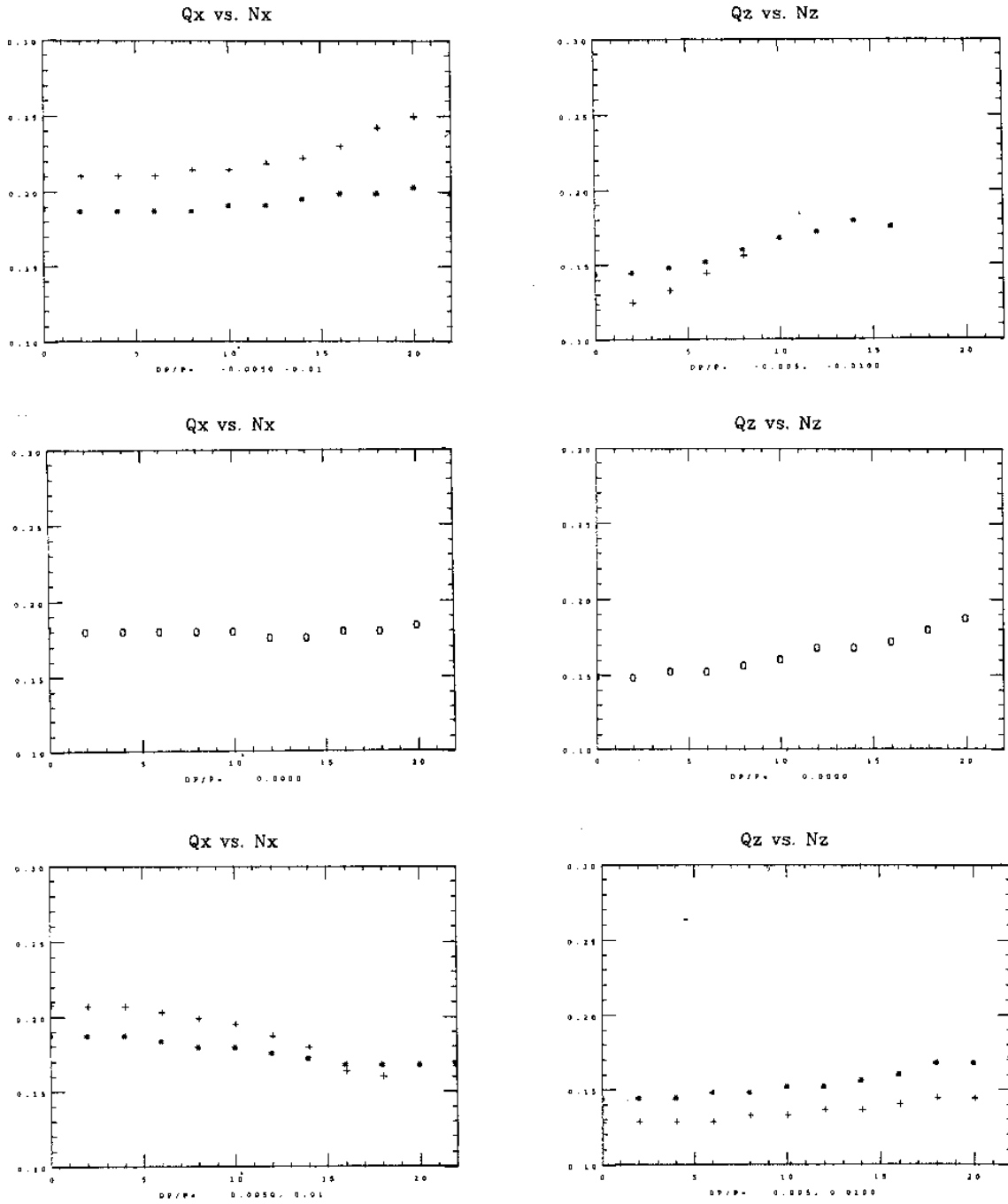


Fig.8a - Main Ring tune dependence on amplitude for different energies.  
 "\*" correspond to  $\pm 0.5\%$ , "+" to  $\pm 1\%$ , and "0" to the nominal energy.

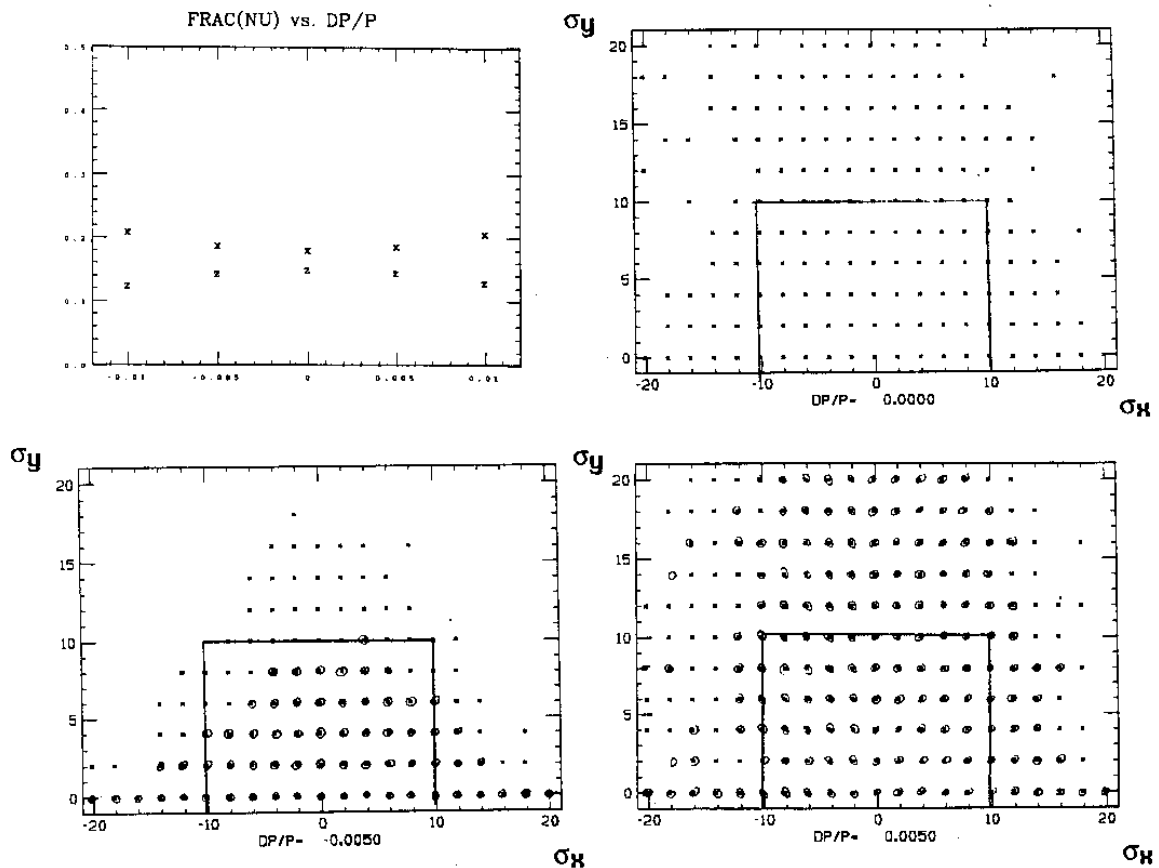


Fig.8b - Main ring tune dependence on momentum and dynamic aperture for different energies.  
 Shaded area in the two last pictures correspond to  $\Delta p/p = \pm 1\%$ .  
 The rectangles delimit the physical aperture.

## REFERENCES

- 1 G. Guignard, "Revised schemes of skew-quadrupoles for solenoid compensation in LEP", LEP-70/75.
- 2 M. Bassetti, J.P. Koutchouk, "The compensation of the solenoidal perturbation (an alternative computation), LEP Note 631, 6 Nov. 1990.
- 3 M. Bassetti et al- "DAΦNE Interaction Region Design" Presented at PAC'93, May 1993, Washington.
- 4 L. Barkov et al., Novosibirsk Project of  $\Phi$ -Meson Factory, Proceedings of Workshop on Physics and Detectors for DAΦNE - Frascati, April 9-12 1991, p.67.
- 5 The FI.NU.DA Collaboration, LNF-93/021(IR), May 1993.
- 6 C. Biscari "DAΦNE Stay-Clear Aperture", Technical Note L-6.
- 7 M.E. Biagini, C. Biscari, S. Guiducci, J. Lu, M.R. Masullo, G. Vignola, "Review of DAΦNE lattices", Technical Note L-9.
- 8 M.E. Biagini, "DAΦNE: a tracking program for the Frascati  $\Phi$ -factory", Technical Note L-7.

## APPENDIX

## OPTICAL PROPERTIES OF SOLENOIDS

In the following we recall some well known properties of quadrupole and solenoid optical effects.

Quadrupoles focus in one plane and defocus in the opposite, while solenoids focus and rotate in both planes. According to the Rotating Frame Method<sup>3</sup> the solenoid effect can be decomposed for each plane in a rotation by the angle:

$$\Theta_{\text{rot}} = \frac{B_z L_s}{2B\rho}$$

( $B_z$  is the longitudinal magnetic field on axis, assumed uniform,  $L_s$  is the total solenoid length and  $B\rho$  is the beam magnetic rigidity) and a focusing in both the radial and the vertical planes, whose strength is given by

$$K_s = \left( \frac{B_z}{2B\rho} \right)^2$$

to be compared with the corresponding quadrupole strength with the same length (rectangular model):

$$K_q = \frac{1}{B\rho} \frac{\delta B}{\delta x}$$

The solenoid is more chromatic by a factor 2 with respect to a quadrupole with the same focusing strength, because of the different energy dependence.

Writing the integrated solenoid focusing strength as function of the rotation angle:

$$K_s L_s = \frac{\Theta_{\text{rot}}^2}{L_s}$$

we notice that while  $\Theta_{\text{rot}}$  depends only on the integral of  $B_z$ , the focusing strength, once fixed  $\Theta_{\text{rot}}$ , is inversely proportional to  $L_s$ . This explains why the focusing properties of the small compensating solenoid are so relevant while those of the detector with the same absolute value of  $\Theta_{\text{rot}}$  are negligible.

This rectangular model is exact only in the limit of an uniform field shape is uniform, which happens when the ratio between the internal radius and the total length is small, or when the magnetic field is cut with iron (like in the DAΦNE detectors).

In a more general case the optical effects of a longitudinal magnetic field can be computed or by tracking or by decomposing it in thin slices, each of them being represented by a rectangular model. The correctness and compatibility of these two approaches has been checked as described before.